Received: 4 September 2023 | *Revised:* 30 December 2023 | *Accepted:* 30 December 2023
DOI: 10.37917/ijeee.21.1.5 *Early View* | *June 2025*

Iraqi Journal for Electrical and Electronic Engineering
Original Article

Open Access
IJEEE University of Basrah College of Engineering

Design and Implementation of the Soft Robot's End-Effecter

Shahad A. Al-Ibadi*, Loai A. T. Al-Abeach, Mohammed A. Al-Ibadi
Computer Engineering Department, College of Engineering, University of Basrah, Basrah, Iraq

Correspondance
*Shahad A. Al-Ibadi
Computer Engineering Department, College of Engineering
University of Basrah, Basrah, Iraq
Email: engpg.shahad.lateef@uobasrah.edu.iq

Abstract
Soft robotics is a modern technique that allows robots to have more capabilities than conventional rigid robots. Pneumatic Muscle Actuators (PMAs), also known as McKibben actuators, are an example of soft actuators. This research covered the design and production of a pneumatic robot end effector. Smooth, elastic, flexible, and soft qualities materials have contributed to the creation of Soft Robot End-Effector (SREE). To give SREE compliance, it needs to handle delicate objects while allowing it to adapt to its surroundings safely. The research focuses on the variable stiffness SREE's inspiration design, construction, and manufacturing. As a result, a new four-fingered variable stiffness soft robot end effector was created. SREE has been designed using two types of PMAs: Contractor PMAs (CPMAs) and Extensor PMAs (EPMAs). Through tendons and Contractor PMAs, fingers can close and open. SREE was tested and put into practice to handle various object types. The innovative movement of the suggested SREE allows it to grip with only two fingers and open and close its grasp with all of its fingers.

Keywords
Soft Robots, Soft Robot End-Effecter (SREE), Contractor Pneumatic Muscle Actuator (CPMA), Extensor Pneumatic Muscle Actuator (EPMA).

I. Introduction

Rigid robots are constructed from tough materials, unlike soft robots, which use soft, lightweight, and responsive materials. Soft robots have modular bodies created of stretchable rubber parts that may combine serially or simultaneously to produce intricate morphologies [1]. Those parts could be constructed from various substances with varying degrees of stiffness [2]. Technological advances in soft components and materials that work well with the soft body have enabled the soft robot to perform autonomously [3]. Parts of a soft robot are often manipulated in two ways, but not exclusively: Tendons (in the form of shape memory alloy actuators or tension wires or threads) may be inserted in soft parts to construct soft robot arms [4], and in a second popular method, channels in a soft material are inflated by pneumatic actuation to produce the desired deformation [5]. Pneumatic Muscle Actuators (PMAs), also known as McKibben actuators, are an example of soft-compliant actuators and consist of elastomer tubes encased in fiber sleeves. The design and production of a pneumatic robot end effector were covered in this chapter. Soft, elastic, flexible, and soft qualities materials have contributed to the Soft Robot End-Effector (SREE) creation. In addition, SREE can handle a variety of objects, including those that are primarily delicate and highly malleable [5]. The inspiration design, construction, and manufacturing of the variable stiffness SREE are first covered in the research. Additionally, A sequence of experiments is proposed to measure the end effector's capabilities at various stiffnesses and explain the concept underlying the recommended end-effector ability to vary stiffness, followed by the related kinematics. Various object types are grasped by SREE. Finally, some concluding remarks are presented.

This is an open-access article under the terms of the Creative Commons Attribution License,
which permits use, distribution, and reproduction in any medium, provided the original work is properly cited.
©2024 The Authors.
Published by Iraqi Journal for Electrical and Electronic Engineering | College of Engineering, University of Basrah.

Fig. 1. Hydrostatically keleton animals.

II. Soft Robot End-Effecter Design Inspiration

Many invertebrates have hydrostatic skeletons, including snails, snakes, and caterpillars. Also, hydrostatic nature is common in marine life, such as jellyfish and sea anemones. Hydrostatically, animals have flexible bodies with limited movement restrictions [6], as shown in Fig.1. These properties are provided by its structure, which consists of an inner chamber filled with an incompressible liquid and a container that is flexible on all sides. Usually, this container consists of the body wall with muscles, making the entire body hydrostatic [7]. A human hand has soft skin with the ability to control grasping stiffness by hand muscles [8]. As a result, it can grasp all types of objects. In addition, it has a large variety of movements with a great degree of stability, precision, strength, and flexibility [9].

Some researchers inspired soft robots from human hand form, skin, and skills, and it used successfully to grasp different types of objects [10]. Various muscles in the human forearm are responsible for moving the fingers by constricting to move tendons. Understanding the kinematics of the hand requires understanding ideas related to muscles and nerves. The source of inspiration for the contractor PMAs is the human muscle itself, which swells when a force must be applied. The proposed SREE forearm design has been inspired by the human forearm, tendons, tensile sensing, and skills of fingers. The use of materials and design will be the primary prerequisite that has been proposed in this chapter.

Based on the technology of the Schunk Anthropomorphic Hand (SAH), as shown in Fig.2 [11], the SREE fingers have been inspired. Three fingers have two degrees of freedom (DoF), and the last one, which was like a thump, has three DoF.

A. Soft Robot End-Effector Design

The PMA structure is the primary part of SREE development. The braided shaded sleeve-covered rubber tubes represent soft robot muscles. Those muscles are used to construct the end effector as actuators. These actuators are constructed in two different ways—one of them as Contractor PMA (CPMA) and the other as Extensor PMA (EPMA). A braided sleeve is used to build the difference between them. The main job of the founding mesh sleeve in contact with a rubber tube is to restrict muscle movement. As a result, the end effector structure will still comprise flexible/soft material with outstanding qualities and high deformation capabilities. Soft actuators are typically arranged in an agonist-antagonist configuration that draws inspiration from biological muscle principles to enable bi-directional actuation [12]. As shown in Table I, CPMAs are built depending on special features such as length and diameter.

Based on Table.I, the CPMA represents the forearm structure of SREE as the same as the human hand structure. Nine CPMAs were arranged into four groups. Each group was responsible for the movement and bending of the SREE fingers. Fabrication includes the process of building SREE out of standard pieces. Standard pieces were: A braided shaded sleeve restrict rubber tubes, and both ends were secured with two types of end caps cylinders; one had a hole for pressure inlet and one for air trapping. This process was utilized to make

Fig. 2. The schunk anthropomorphic hand (SAH).

TABLE I.
Specifications of CPMA and EPMA Design

PMA	Features				
	Tube Length	Tube Diameter	Sleeve Length	Sleeve Diameter	Total length with both caps
CPMA	230 mm	17 mm	230 mm	17 mm	250 mm
EPMA	150 mm	17 mm	400 mm	17 mm	182 mm

Fig. 3. Components of PMA.

CPMAs, as shown in Fig.3. The SREE structure consists of three bases. AUTOCAD software was used to design the first base, as shown in Fig.4.

The first base was responsible for holding the CPMA groups. A 3D printer and a CNC machine were used to produce the CPMA base, and it was constructed from three layers of acrylic material, a 2.5 mm thickness for each one. In addition, this base had two types of holes; one was used for fixing aluminum end caps cylinders. The other holes were used for passing three metal shaft screws that fixed all three bases together.

The task of the aluminum end caps is to hold the CPMAs and allow to pass the compressed air through the holes inside them, as shown in Fig.5A and Fig.5B. The end cap's base dimensions were selected to be (126*137*7.5) mm. The aluminum cylinders had holes in the center to fixed pressure inlets. The dimensions of the aluminum end caps were (37 mm) in length and (17 mm) in diameter. The nine CPMAs are

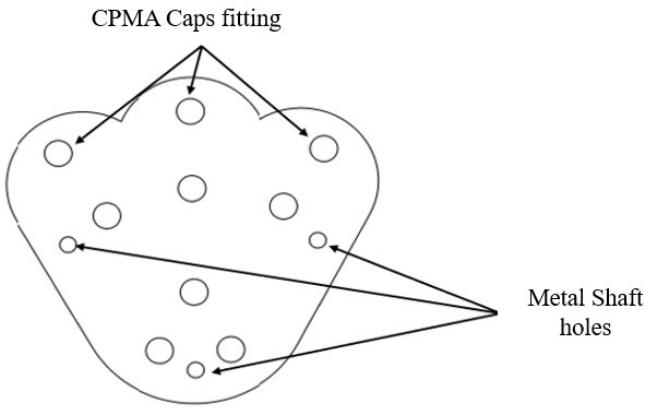

Fig. 4. Sketch of CPMA's base structure.

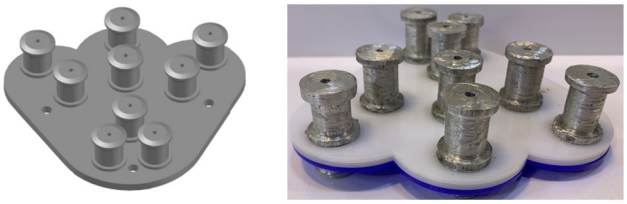

Fig. 5. The first base structure of SREE (A) 3D design, (B) Practical base.

fitted to these aluminum cylinders.

The second end caps were designed in AutoCAD software and produced by a 3D printer using Polylactic Acid (PLA) material. The dimensions of the end caps were (37 mm) in length and (17 mm), see Fig.6. The tendons were tied to these caps from their end.

Fig.7 below shows the second base sketch diagram used to fix nine slide potentiometer sensors.

AutoCAD software also designed and produced this base with a 3D printer machine, as shown in Fig.8A and Fig.8B.

The third base sketch illustrated in Fig.9 demonstrates the fitting of holes and displacement sensor regions based on the sketch below.

The practical model of the third base has been designed by AutoCAD software, as shown in Fig.10A and printed in a 3D printer machine, as shown in Fig.10B. The practical base has another side responsible for carrying the EPMAs.

B. Soft Fingers Design

The SREE must be soft to interact with people safely or to bend around the object to grip. The idea of soft manipulators was the foundation for the end effector created in this study. EPMA makes up each of the four fingers with different DoF. In addition, EPMAs were built depending on unique features

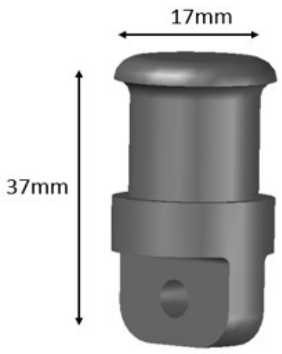

Fig. 6. Second CPMA end cap structure.

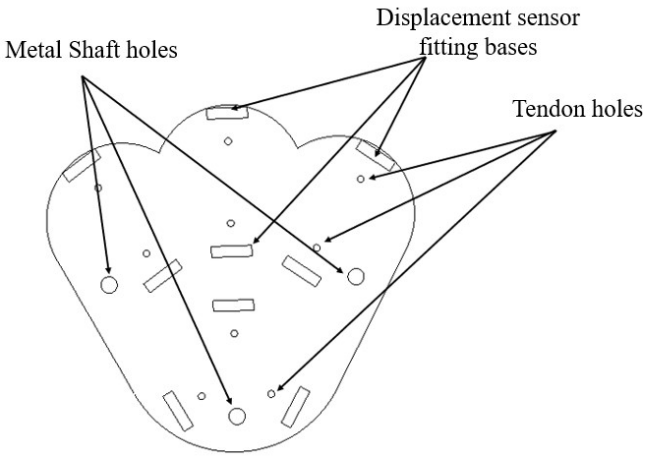

Fig. 7. Sketch of second base structure.

such as length and diameter to represent extending muscles as fingers to the SREE, as shown in Table.I.

Based on the EPMA table specifications, EPMAs are represented as the fingers of SREE. SREE consisted of four EPMAs as fingers. The EPMA was constructed based on EPMA specifications and as components shown previously in Fig.3.

A braided shaded sleeve covered the rubber tube. Both EPMA ends were secured with two types of end caps: one aluminum fabricated for pressure inlet. The other end cap for air trapping is printed with a 3D printer according to the dimensions of the rubber tubes. Three tendons were attached around the EPMA. Tendons pass through loops added along the EPMA to ensure the EPMA remains in a straight shape during the operation work. EPMA's role is to be fingered in the proposed SREE. These fingers bend according to the CPMA actuation magnitude and take the shape of the pressure applied. The stiffness of the suggested SREE can be changed by varying the pressure in the EPMA and CPMAs. Slight pressure on the EPMAs and CPMAs produces a very flexible SREE.

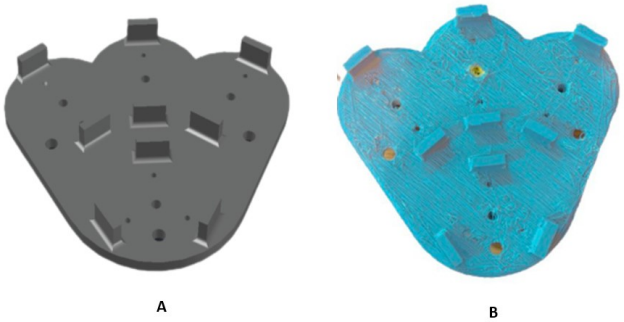

Fig. 8. Second base structure for SREE (A) 3D design, (B) Actual base.

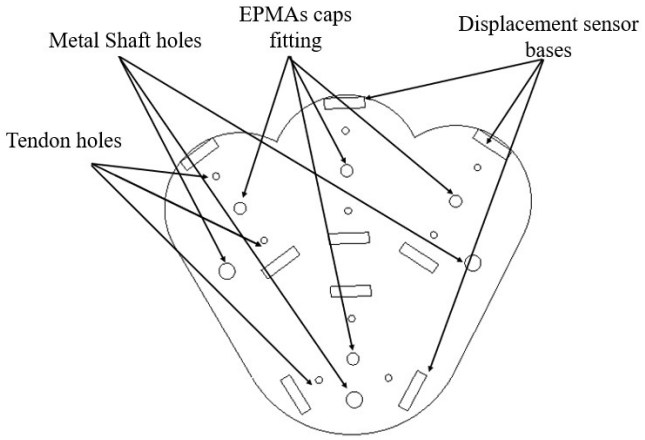

Fig. 9. Sketch of third base structure.

The soft fingers are fitted on the third base. This base has three types of holes; the first type is used for passing aluminum end caps. The second type is used for the metal shaft screw, and other holes are used to pass the fingers' tendons, see Fig.11. The aluminum caps are fitted through the EPMA holes. The aluminum caps are used to hold EPMAs and used to pass the air pressure through them. Three aluminum caps were designed with a little distance between them. On the other hand, the last aluminum cap was allocated far from the others to carry the thump finger as shown in Fig.11.

III. Assembling The Soft Robot End-Effecter

The proposed SREE has been constructed from three bases, as previously demonstrated. To test the functionality of the aforementioned SREE, the forearm and soft fingers are used to create the modules of the SREE. The linear rails are made of metal to ensure the components are fixed well together. Fig.12 illustrates the first structure of the assembly process. The aluminum mount caps are placed and used to fix nine CPMAs of the same size on the first base. In addition, nine

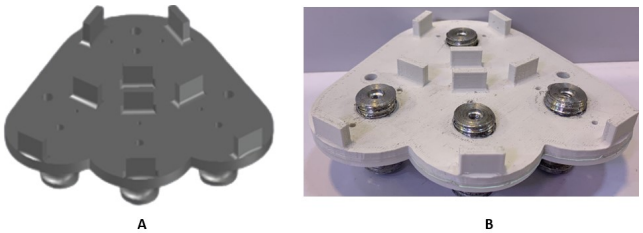

Fig. 10. Third base structure of the SREE (A) 3D design, (B) Practical base.

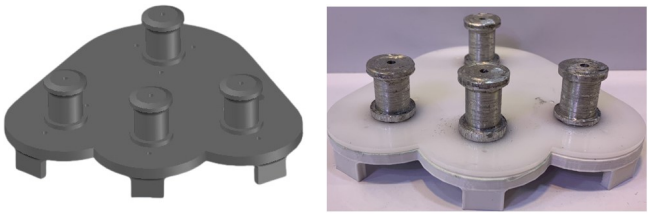

A B

Fig. 11. The third base structure of the SREE (A) 3D design, (B) Practical base.

displacement sensors were fixed between the second and the third bases. Finally, four sizes of EPMAs were fitted to the aluminum mounts fixed on the last base. A 3D model SREE design is represented in Fig.13.

The forearm of the SREE is constructed with nine CPMAs divided into four groups. Three groups have two actuators that provide bending power to the three fingers. The remaining group has three actuators that provide bending power to the thump finger. Fig.14 demonstrates the model of the actual structure.

The nine CPMAs have nine tendons (threads) linked into the free ends of them, which pass through the second and third bases. In addition, through the 10 k■ sliding potentiometer sensors' central terminals, which are fixed between these bases. Each CPMA tendon was attached to a single potentiometer. The pulling force from the CPMAs is transferred to the soft fingers via these tendons. These nine tendons were attached around the soft fingers. As a result, tendons would control the fingers bending. Three fingers had two couples of tendons passed through the braided sleeve shell. In addition, three couples of tendons are attached around the thump finger. An angle of 120 degrees separated these tendons to achieve movement. Slide potentiometer sensors were used to provide

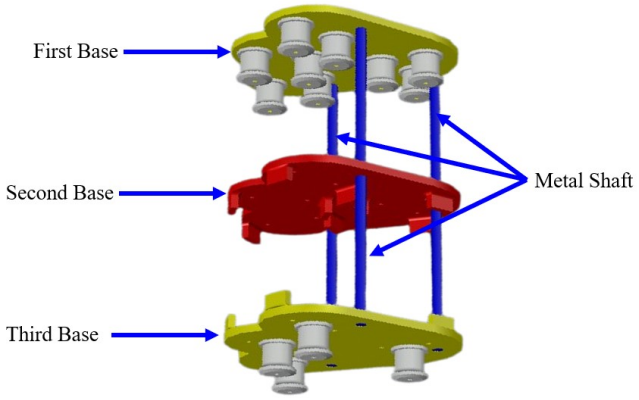

Fig. 12. RA 3D first structure of the SREE.

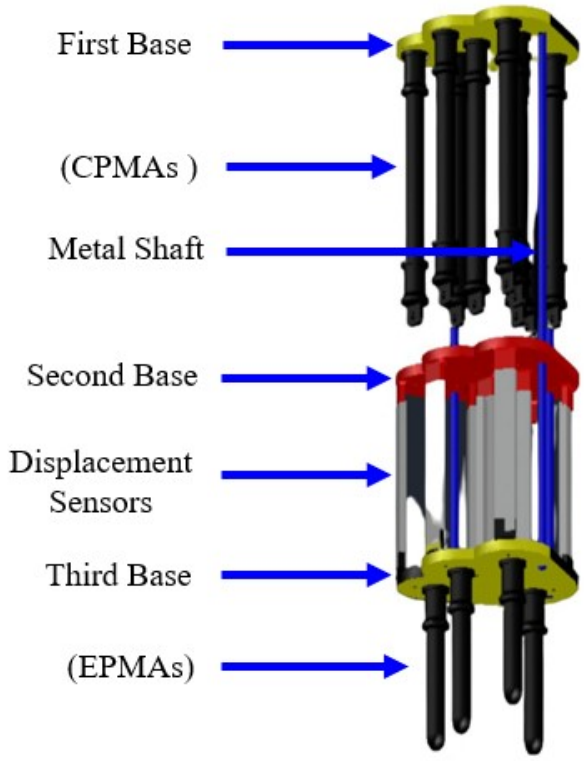

Fig. 13. A 3D structure design of the SREE with CPMAs and EPMAs.

measured displacement data via Arduino. These data were produced by the CPMA pulling force. Furthermore, the measured displacement data are used as feedback for the position control system.

Altogether, there are thirteen Pneumatic Muscle Actuators (PMAs): nine CPMAs, and the other four are EPMAs. In addition, nine air pipes and air inlets are connected to CPMA aluminum caps. Two air pressure regulators were used to insert pressure inside the CPMAs and EPMAs via air pipes. A solenoid valve was used to control the pressures inside CPMAs. Otherwise, The EPMAs' air pressure regulator had constant pressure (150 kPa). A solenoid valve had four output ports joined with CPMA inlets, which were used to control air Fill/ Vent. As shown in Fig.15.

The MATRIX 3-3 solenoid valve (MK 754.8E1D2XX) channels series solenoid valve is controlled airflow. The benefits of this valve include its small size, quick response time, immunity to vibrations and frequency work, low absorbed power, repeatability, precision, and extended operational life [13]. When controlling the position of the SREE actuators with Fill/Vent solenoid valves, the controller output must be resolved into each pulse valve. It had twelve wires, four wires for GND, and the others were distributed as pairs (one for

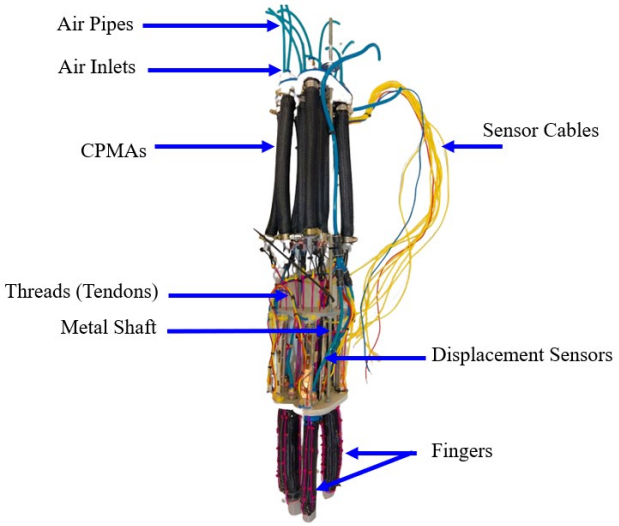

Fig. 14. Final practical structure of the SREE.

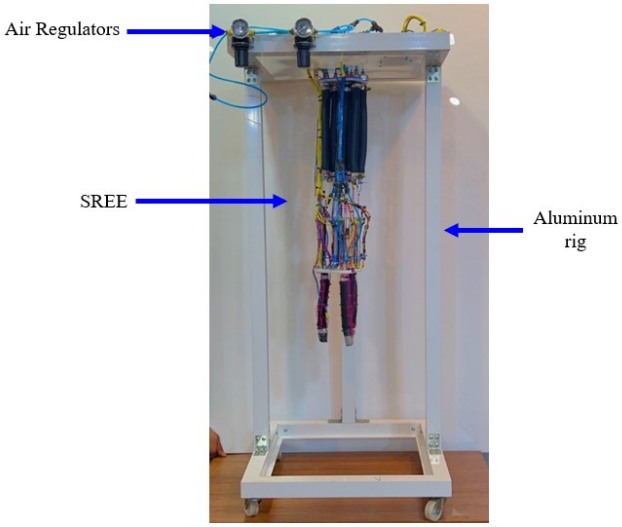

Fig. 16. The proposed SREE.

fill and the second for vent). An Arduino microcontroller linked to MATLAB operated the matrix valve with PWM signals. Each valve's port had three wires to control PWM signals. PWM signals were used to control the airflow rate inside and outside each CPMA. The matrix solenoid valve requires 12VDC to operate the Fill/Vent, but the output pin of the Arduino board had only 5VDC. Therefore, a driver circuit should be used. Each element of the proposed SREE was assembled inside an aluminum rig, as shown in Fig.16.

IV. Stiffness in Soft Robot End-Effecter

Variable stiffness in soft robots aims to interact safely with a human and fragile object. Consequently, designing SREE that can vary its stiffness would represent a significant advance in the creation of robots in the future. Variance in robot stiffness could be done by changing the air pressure in the PMAs. Increasing pressure on the EPMAs can stiffen the fingers. Furthermore, to keep the finger in the same position, the EPMA air pressure is increased, and the air pressure in the CPMAs must likewise be increased.

Moreover, the overall stiffness of the finger will rise due to the tremendous pressure on the CPMAs and EPMAs. Otherwise, applying low pressure inside CPMAs and EPMAs allows for very flexible SREE. Moreover, the SREE became noticeably stiffer if considerable pressure was applied to both PMAs. When precise control is required, a stiffer end effector is preferable. Based on the research, the suggested SREE can theoretically be configured in endless ways to alter stiffness—experiments of variable stiffness [10].

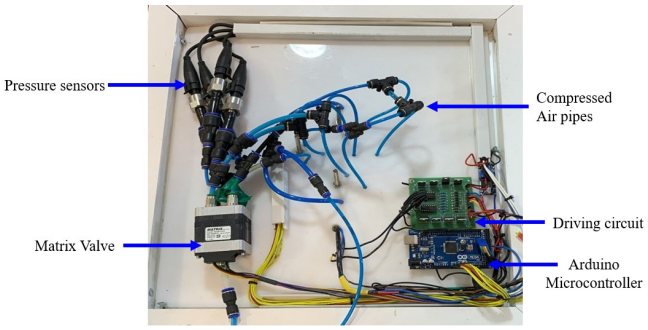

Fig. 15. Controller hardware system.

A. Stiffness measurement in the proposed SREE:

To investigate the stiffness in SREE, a practical experiment was conducted using four various levels of pressure applied to both CPMAs and EPMAs. The amount of pressure inside both actuators types leads to getting the required length of fingers. The length of EPMAs was decreased by increasing the air pressure inside CPMAs that transfer by tendons. The setting of a practical experiment was demonstrated in Fig.17. Fig.17 shows how the SREE's finger is pointed downward by suspending the end effector vertically. A tendon was linked to the fingertip and transferred to a load through a pulley. The fingertip moves laterally due to increased horizontal force acting on it as the load is raised. Based on this displacement, the lateral finger bending stiffness might be computed for various EPMA tensions. A moveable aluminum pulley is responsible for the cable's direction and the force applied. Each step involved adjusting the height of the pulley. A laser pointer

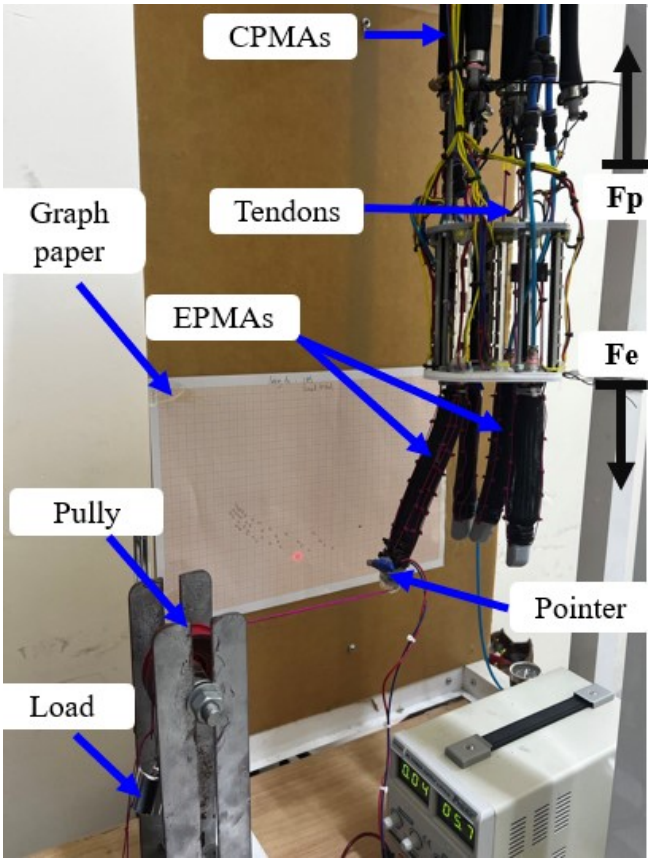

Fig. 17. The setting of practical stiffness experiment.

was attached to the thumb finger to indicate the displacement onto a piece of graph paper by focusing the laser beam onto a target. CPMAs were completely vented before the experiment began, and the EPMAs' pressure was then manually adjusted to the necessary test pressure using the manual regulator.

The finger/EPMA will lengthen due to the force (Fe) produced due to weight hang. Pull force (Fp) in the EPMA was produced when the second manual regulator was employed to increase pressure in the CPMA's. EPMA active length was 150 mm. It became shorter due to pulling forces acting antagonistically force (Fe) through the tendons. The EPMA length was adjusted to match the requirements for the bending stiffness studies mentioned below by increasing the air pressure in the CPMAs. The thumb moved in all directions according to the amount of (Fp) by moving three CPMAs that actuated bending through the extending tendons.

On the other hand, the other fingers move in just two directions (open and close) according to the amount of (Fp) by moving two CPMAs that actuate bending through tendons extending from them. EPMA became shorter due to these forces acting antagonistically on Fe. The EPMA length was adjusted to match the requirements of the bending stiffness studies mentioned below by raising the CPMA's tension.

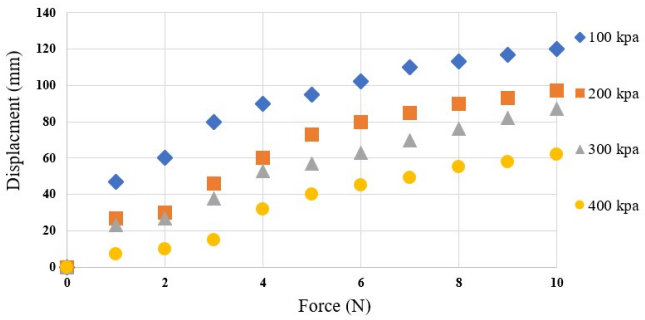

Fig. 18. Displacement Vs. Force at various pressures for finger length (145 mm).

B. *Practical experiments to calculate bending stiffness properties:*

The first investigation experiment on the bending stiffness was carried out with a soft finger/EPMA length of 145 mm. The EPMA pressure was placed at 100 kPa, and the CPMA pressure was subsequently increased to 50 kPa until the finger/EPMA length was lowered to 145 mm. After applying lateral force to the soft fingertip from (0.98 to 9.98)N with increments of '0.98 N' each step, the finger's adjacent displacement was measured. EPMA pressures (200, 300, and 400) kPa are used in experiments and CPMA pressures of (60, 90, and 100) kPa respectively. The primary purpose is to maintain the finger length at 145 mm. Fig.18 demonstrates the displacement of the EPMA versus the lateral load at different pressures. The early observation is that the stiffness increased by applying more pressure to the SREE's EPMAs and CPMAs.

The practical experiment was repeated three times to improve the dependability of the results. An average value of the results is shown in Fig.19.

As expected, the finger's lateral displacement rises as the force increases. Additionally, it could be seen that the lateral force was required to move the fingertip differently when the EPMA was under higher pressure than it was under lower pressure. A bending stiffness value could be calculated for each experiment using the above-mentioned experimental findings. The experimental results were approximated linearly to achieve the result as shown in Fig.19.

The compliance can be calculated by:

$$Compliness = \frac{Displacment(mm}{Force(N)} \quad (1)$$

The stiffness of the fingers was calculated according to the following equation:

$$Compliness = \frac{Displacment(mm)}{Compliness} \quad (2)$$

Fig.20 illustrates the Stiffness vs pressure characteristics of the proposed SREE at length (145 mm).
According to the preceding Figure, an increase in CPMA pressure at the finger leads the soft finger stiffness to increase for a soft finger length of 145 mm. The second practical experimental investigation on bending stiffness was carried out with a finger-actuated length of 140 mm.
The final experiment was repeated after changing the finger-actuated length to 130 mm. Fig.21 shows the bending stiffness at 130 mm, 140 mm, and 145 mm of the EPMA/finger.

V. The Soft Robot End-Effector's Finger Kinematics

Analyzing the finger's/EPMA's kinematics is essential to determine the location of each fingertip on the proposed SREE. The location of the EPMA's tip concerning the base is determined by the length of the CPMAs, which are uniformly distributed around EPMAs via tendons. The EPMAs bend and produce a radius that is a constant curve with an arc as a result of the shortening of the CPMAs. Based on [14], the length of the arc is determined by the angle between the two ends of the EPMAs, as shown in Fig.22 below.
Godage looked into SREE's kinematics with three expanding actuators [15]. The pneumatic finger's behavior may be predicted using a similar general methodology. Four features describe the location of the finger's end concerning its base. The length of the arc generated isL_arc, the radius formed is

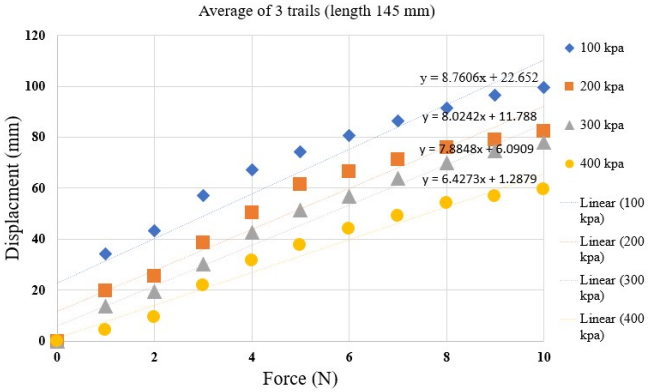

Fig. 19. Average of three practical result and Linear approximation and actual stiffness of finger length 145 mm.

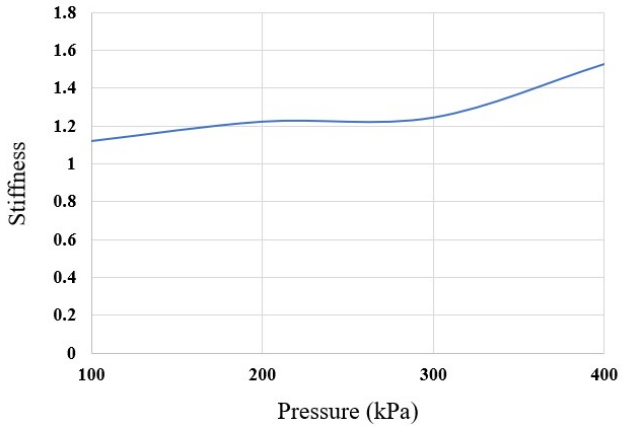

Fig. 20. Linear approximation and actual stiffness of finger length 145mm.

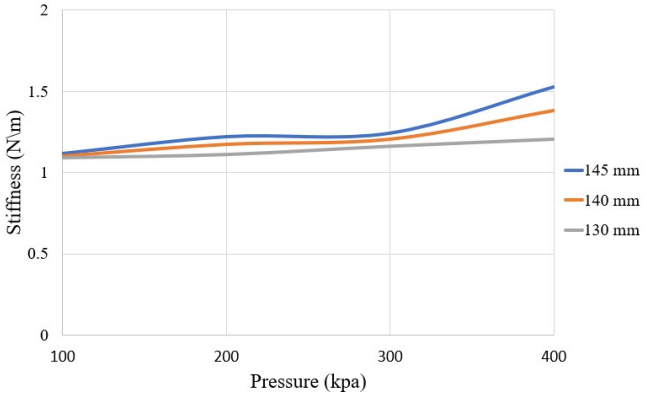

Fig. 21. The finger bending stiffness at 130mm,140mm, and 145mm lengths.

λ, and the angle between the end of the portion point and the base coordinate edge is θ. The angle ϕ represents the angular dislocation between the two ends of the finger. The four equations below give the kinematics of the three fingers shown in Fig.22A.

$$\lambda = \frac{(L_1 + L_2)r_0}{\sqrt{L_1^2 + L_2^2 - L_1 L_2}} \quad (3)$$

$$\phi = \frac{\sqrt{L_1^2 + L_2^2 - L_1 L_2}}{2r_0} \quad (4)$$

$$\theta = \tan^{-1}\left(\frac{\sqrt{2}(L_2 - L_1)}{L_2 - 2L_1}\right) \quad (5)$$

$$L_{arc} = \lambda\phi \quad (6)$$

Equations (3), (4), and (6) can be used to yield the following result as the finger's length:

$$L_{finger} = \frac{L_1 + L_2}{2} \tag{7}$$

The finger was made using the EPMA, whose length is designated as L_finger. The individual contractions of the two CPMAs are $L_1 and L_2$, and the distance between the CPMAs and the finger's central axis is r_0. However, this measurement is not required to determine the total length L. Despite being fashioned as an EPMA, the finger in this piece has a variable diameter since it expands as its diameter falls. As a result, the tendons' distance from the EPMA's central equals the radius of the manufactured EPMA. L *and* r_0 of EPMA are founded using the formula below:

$$L = \cos\theta_B \tag{8}$$

$$r_0 = \frac{b\sin\theta_B}{2n\pi} \tag{9}$$

Where: b is the distance of a single fiber, n is the fibers loop around the EPMA's circle, and θ_B is the braid's angle with respect to the axis that runs through the middle of the EPMA. By combining these two equations with regard to θ_B Band take the place into Eq.9, the following equation links the length of the three tendons to the EPMA radius:

$$r_0 = \frac{\sqrt{b^2 - L^2}}{2n\pi}$$

$$r_0 = \frac{\sqrt{b^2 - \frac{L_1+L_2}{2}^2}}{2n\pi}$$

$$r_0 = \frac{\sqrt{4b^2 - (L_1+L_2)^2}}{4n\pi} \tag{10}$$

The position of the EPMA's tip concerning the base can then be found by integrating Eq.10, which depends on the tightening of the two CPMAs (L_1 *and* L_2). On the other hand, the thump finger bending depends on three CPMAs, as shown in Fig.22B. The proposed thump finger is the same as the fingers in the research [16]. As a result, the same equations are used to calculate thump finger kinematics.

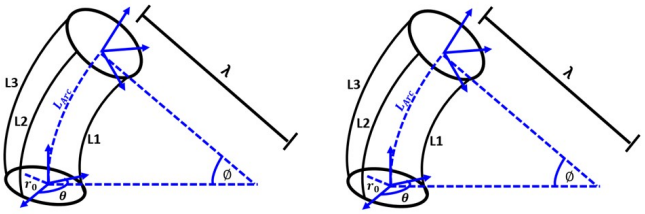

Fig. 22. The kinematics of (A) Three fingers and (B) Thump finger.

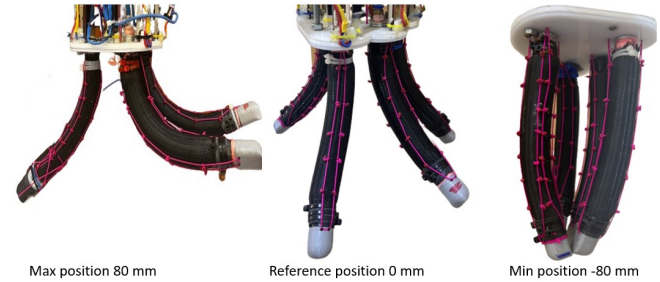

(a)

(b)

Fig. 23. For the sub-figures.

It should be noted that this analysis is only valid when the finger is not being affected by other forces, such as when the SREE is not grasping anything. Because the fingers are delicate, applying external forces would cause them to deform very complicatedly, necessitating a more sophisticated kinematic/dynamic study.

VI. Soft Robot End Effector: Performance Evaluation

Experiments have defined the performance of the suggested SREE. The length of the fingers is changed by applying air pressure through a solenoid valve to the CPMA actuators. A constant pressure amount (150 kPa) is applied to the fingers. Lengths of fingers alter as pressure increases or decreases in CPMAs. The results of the grabbing experiments are shown in Fig.23. Fig.23A shows the finger's position movement when the maximum opens at 80 mm, then it stops at 0 mm position, and the minimum closes at -80mm. As can be seen in Fig.23B, the SREE was discovered to be capable of gripping various soft objects with multiple sizes, weights, and forms.

The SREE can grasp in addition to closing and opening with four fingers. It can also handle objects with just two fingers with the help of a thumb finger and any finger that meets, as

Fig. 24. Handling different types of objects with just two fingers.

shown in Fig.24.

VII. Conclusion

A new four-fingered variable stiffness soft robot end effector was created using an improved design. Through tendons and the use of CPMAs, fingers can close and open. This decreases the proposed end effector's design and control operation complexity, as well as the effort and time required to implement it. Two CPMAs were used to bend each finger, and one EPMA was used to construct the finger. Three CPMAs move the thumb finger. In the revised design, the tendon cables were arranged in a better way. This configuration made it easier for the fingers to flex while the end effector was opening and shutting. The design utilizes an unusual mixture of pneumatic muscles that contract and expand in opposition to each other. By regulating the pressure in CPMAs, the end SREE's stiffness may be changed without altering the position of the fingers. According to an empirically supported theory, this enables the suggested gripper to change the location and stiffness of the fingers independently. The fingers' forward kinematics have been illustrated. SREE has been put through evaluating and operates with a variety of object kinds.

Conflict of Interest

The authors have no conflict of relevant interest to this article.

References

[1] M. A. Robertson and J. Paik, "New soft robots really suck: Vacuum-powered systems empower diverse capabilities," *Science Robotics*, vol. 2, no. 9, p. eaan6357, 2017.

[2] S. A. Al-Ibadi, L. A. T. Al Abeach, and M. A. A. Al-Ibadi, "Soft robots: Implementation, modeling, and methods of control," *Indonesian Journal of Electrical Engineering and Informatics (IJEEI)*, vol. 11, no. 1, pp. 194–209, 2023.

[3] G. Giordano, M. Carlotti, and B. Mazzolai, "A perspective on cephalopods mimicry and bioinspired technologies toward proprioceptive autonomous soft robots," *Advanced Materials Technologies*, vol. 6, no. 12, p. 2100437, 2021.

[4] C. Yang, S. Geng, I. Walker, D. T. Branson, J. Liu, J. S. Dai, and R. Kang, "Geometric constraint-based modeling and analysis of a novel continuum robot with shape memory alloy initiated variable stiffness," *The International Journal of Robotics Research*, vol. 39, no. 14, pp. 1620–1634, 2020.

[5] H. K. Yap, H. Y. Ng, and C.-H. Yeow, "High-force soft printable pneumatics for soft robotic applications," *Soft Robotics*, vol. 3, no. 3, pp. 144–158, 2016.

[6] A. A. Calderón, J. C. Ugalde, L. Chang, J. C. Zagal, and N. O. Pérez-Arancibia, "An earthworm-inspired soft robot with perceptive artificial skin," *Bioinspiration & biomimetics*, vol. 14, no. 5, p. 056012, 2019.

[7] S. Kim, C. Laschi, and B. Trimmer, "Soft robotics: a bioinspired evolution in robotics," *Trends in biotechnology*, vol. 31, no. 5, pp. 287–294, 2013.

[8] R. Deimel and O. Brock, "A novel type of compliant and underactuated robotic hand for dexterous grasping," *The International Journal of Robotics Research*, vol. 35, no. 1-3, pp. 161–185, 2016.

[9] N. Elango and A. A. M. Faudzi, "A review article: investigations on soft materials for soft robot manipulations," *The International Journal of Advanced Manufacturing Technology*, vol. 80, pp. 1027–1037, 2015.

[10] L. A. T. Al Abeach, *Pneumatic variable stiffness soft robot end effectors*. University of Salford (United Kingdom), 2017.

[11] J. Rosell, R. Suárez, C. Rosales, and A. Pérez, "Autonomous motion planning of a hand-arm robotic system based on captured human-like hand postures," *Autonomous Robots*, vol. 31, no. 1, pp. 87–102, 2011.

[12] S. A. Al-Ibadi, L. A. Al-Abeach, and M. A. Al-Ibadi, "Experimental modeling of pneumatic muscle actuator," in *2022 Iraqi International Conference on Communication and Information Technologies (IICCIT)*, pp. 153–158, IEEE, 2022.

[13] H. Al-Fahaam, S. Nefti-Meziani, T. Theodoridis, and S. Davis, "The design and mathematical model of a novel variable stiffness extensor-contractor pneumatic artificial muscle," *Soft robotics*, vol. 5, no. 5, pp. 576–591, 2018.

[14] L. Al Abeach, S. Nefti-Meziani, T. Theodoridis, and S. Davis, "A variable stiffness soft gripper using granular jamming and biologically inspired pneumatic muscles," *Journal of Bionic Engineering*, vol. 15, pp. 236–246, 2018.

[15] I. S. Godage, D. T. Branson, E. Guglielmino, G. A. Medrano-Cerda, and D. G. Caldwell, "Shape function-based kinematics and dynamics for variable length continuum robotic arms," in *2011 IEEE International Conference on Robotics and Automation*, pp. 452–457, IEEE, 2011.

[16] L. A. Al Abeach, S. Nefti-Meziani, and S. Davis, "Design of a variable stiffness soft dexterous gripper," *Soft robotics*, vol. 4, no. 3, pp. 274–284, 2017.